Extraction of GPDs from fits to DVCS observables

Silvia Niccolai (IPN Orsay)

(on behalf of Michel Guidal,

in collaboration with Raphael Dupré and Marc Vanderhaeghen)

INSTITUT DE PHYSIQUE NUCLÉAIRE ORSAY

Deeply Virtual Compton Scattering and GPDs

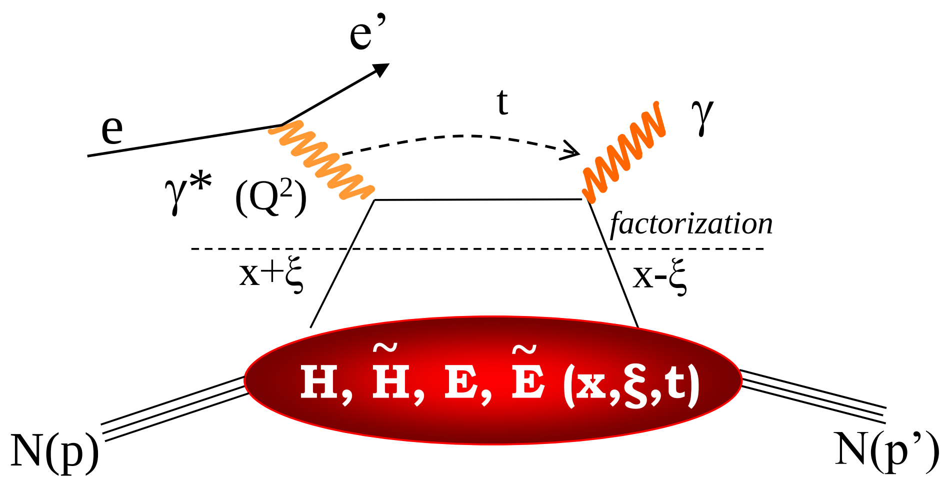

- $Q^2 = -(e-e')^2$
- $x_B = Q^2/2M\nu \quad \nu = E_e - E_{e'}$
- $x+\xi$, $x-\xi$ longitudinal momentum fractions
- $t = \Delta^2 = (p-p')^2$
- $\xi \cong x_B/(2-x_B)$

« **Handbag** » factorization valid in the **Bjorken regime**: **high Q^2, ν (fixed x_B), $t \ll Q^2$**

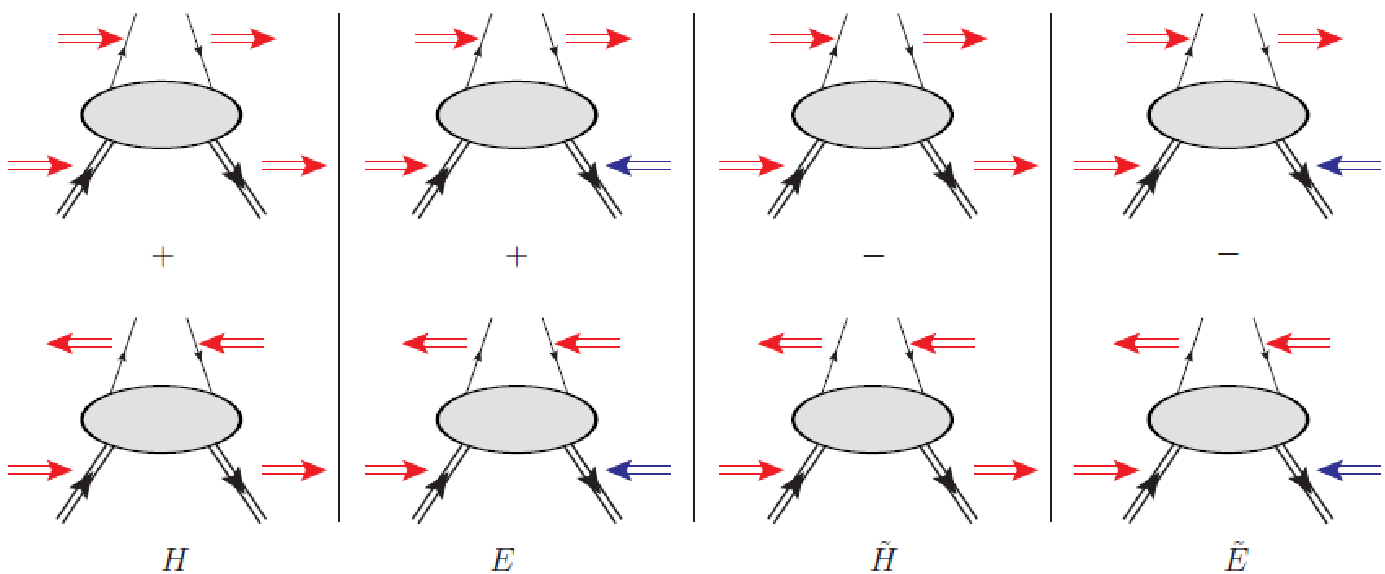

GPDs: Fourier transforms of ***non-local, non-diagonal*** *QCD operators*

At leading order QCD, twist 2, chiral-even (quark helicity is conserved), quark sector
→ **4 GPDs for each quark flavor**

conserve nucleon spin	**Vector: H (x,ξ,t)**	**Axial-Vector: $\tilde{H}$ (x,ξ,t)**
flip nucleon spin	**Tensor: E (x,ξ,t)**	**Pseudoscalar: $\tilde{E}$ (x,ξ,t)**

Properties and "virtues" of GPDs

$$\int H(x,\xi,t)dx = F_1(t) \quad \forall\xi$$
$$\int E(x,\xi,t)dx = F_2(t) \quad \forall\xi$$
$$\int \tilde{H}(x,\xi,t)dx = G_A(t) \quad \forall\xi$$
$$\int \tilde{E}(x,\xi,t)dx = G_P(t) \quad \forall\xi$$

Link with **FFs**

$$H(x,0,0) = q(x)$$
$$\tilde{H}(x,0,0) = \Delta q(x)$$

Forward limit: **PDFs** (not for E, Ẽ)

Nucleon tomography

$$q(x,\mathrm{b}_\perp) = \int_0^\infty \frac{d^2\Delta_\perp}{(2\pi)^2} e^{i\Delta_\perp \mathrm{b}_\perp} H(x,0,-\Delta_\perp^2)$$

$$\Delta q(x,\mathrm{b}_\perp) = \int_0^\infty \frac{d^2\Delta_\perp}{(2\pi)^2} e^{i\Delta_\perp \mathrm{b}_\perp} \tilde{H}(x,0,-\Delta_\perp^2)$$

M. Burkardt, PRD 62, 71503 (2000)

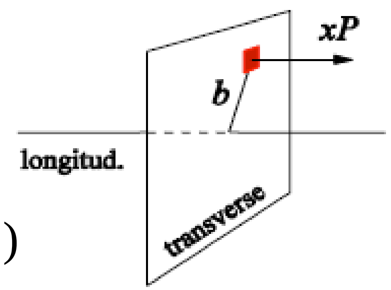

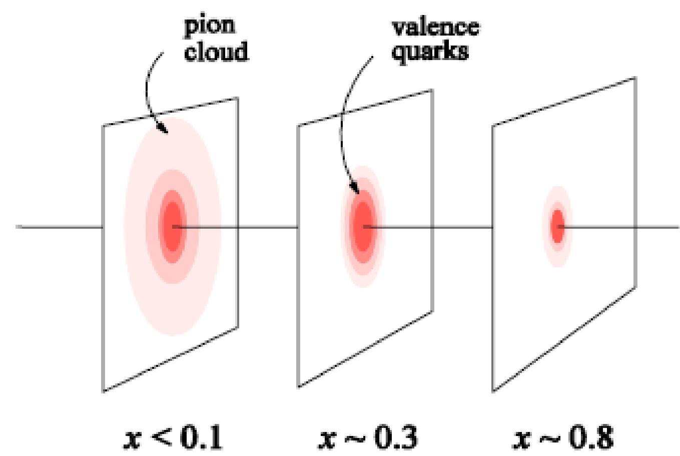

Quark angular momentum (Ji's sum rule)

$$\boxed{\frac{1}{2}\int_{-1}^{1} x dx (H(x,\xi,t=0) + E(x,\xi,t=0)) = J = \frac{1}{2}\Delta\Sigma + \Delta L}$$

X. Ji, Phy.Rev.Lett.78,610(1997)

Nucleon spin: $\frac{1}{2} = \underbrace{\frac{1}{2}\Delta\Sigma + \Delta L}_{J} + \Delta G$

Intrinsic spin of the quarks $\Delta\Sigma \approx 25\%$

Intrinsic spin on the gluons $\Delta G \approx 0$ (??)

Orbital angular momentum of the quarks ΔL ?

Accessing GPDs through DVCS

$$T^{DVCS} \sim P\int_{-1}^{+1} \frac{GPDs(x,\xi,t)}{x\pm\xi}dx \pm i\pi GPDs(\pm\xi,\xi,t) + \ldots$$

$$Re\mathcal{H}_q = e_q^2 P\int_0^{+1}\left(H^q(x,\xi,t) - H^q(-x,\xi,t)\right)\left[\frac{1}{\xi-x} + \frac{1}{\xi+x}\right]dx$$

$$Im\mathcal{H}_q = \pi e_q^2\left[H^q(\xi,\xi,t) - H^q(-\xi,\xi,t)\right]$$

σ(eN ⟶ eNγ) =

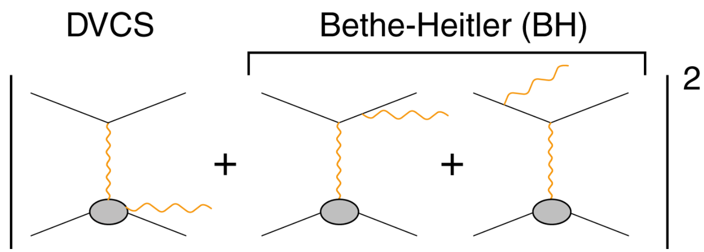

$$\sigma \sim \left|T^{DVCS} + T^{BH}\right|^2$$

$$\Delta\sigma = \sigma^+ - \sigma^- \propto I\left(DVCS \cdot BH\right)$$

Proton Neutron

Polarized beam, unpolarized target:

$\Delta\sigma_{LU} \sim \sin\phi\ \mathrm{Im}\{F_1\mathcal{H} + \xi(F_1+F_2)\tilde{\mathcal{H}} - kF_2\mathcal{E} + \ldots\}$ ⇨ $Im\{\mathcal{H}_p, \tilde{\mathcal{H}}_p, \mathcal{E}_p\}$, $Im\{\mathcal{H}_n, \tilde{\mathcal{H}}_n, \boldsymbol{\mathcal{E}}_n\}$

Unpolarized beam, longitudinal target:

$\Delta\sigma_{UL} \sim \sin\phi \mathrm{Im}\{F_1\tilde{\mathcal{H}} + \xi(F_1+F_2)(\mathcal{H} + x_B/2\mathcal{E}) - \xi kF_2\tilde{\mathcal{E}}\}$ ⇨ $Im\{\boldsymbol{\mathcal{H}}_p, \tilde{\boldsymbol{\mathcal{H}}}_p\}$, $Im\{\boldsymbol{\mathcal{H}}_n, \mathcal{E}_n\}$

Polarized beam, longitudinal target:

$\Delta\sigma_{LL} \sim (A+B\cos\phi)\mathrm{Re}\{F_1\tilde{\mathcal{H}} + \xi(F_1+F_2)(\mathcal{H} + x_B/2\mathcal{E}) + \ldots\}$ ⇨ $Re\{\boldsymbol{\mathcal{H}}_p, \tilde{\boldsymbol{\mathcal{H}}}_p\}$, $Re\{\boldsymbol{\mathcal{H}}_n, \mathcal{E}_n\}$

Unpolarized beam, transverse target:

$\Delta\sigma_{UT} \sim \cos\phi\sin(\phi_s - \phi)\mathrm{Im}\{k(F_2\mathcal{H} - F_1\mathcal{E}) + \ldots\}$ ⇨ $Im\{\boldsymbol{\mathcal{H}}_p, \boldsymbol{\mathcal{E}}_p\}$, $Im\{\boldsymbol{\mathcal{H}}_n\}$

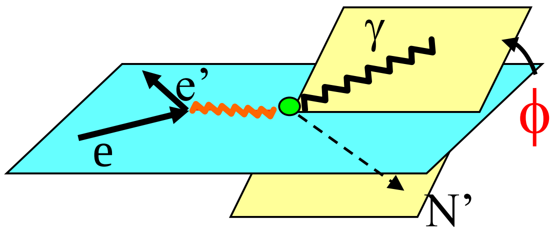

Twist-2 approximation ($-t \ll Q^2$)

$\xi = x_B/(2-x_B)$ $k = -t/4M^2$

8 GPDs-related quantities are accessible from DVCS: (sub-)Compton Form Factors

$$H_{\mathrm{Re}}(\xi,t) \equiv \mathcal{P}\int_0^1 \mathrm{d}x\,[H(x,\xi,t) - H(-x,\xi,t)]\,C^+(x,\xi)$$

$$E_{\mathrm{Re}}(\xi,t) \equiv \mathcal{P}\int_0^1 \mathrm{d}x\,[E(x,\xi,t) - E(-x,\xi,t)]\,C^+(x,\xi)$$

$$\tilde{H}_{\mathrm{Re}}(\xi,t) \equiv \mathcal{P}\int_0^1 \mathrm{d}x\left[\tilde{H}(x,\xi,t) + \tilde{H}(-x,\xi,t)\right]C^-(x,\xi)$$

$$\tilde{E}_{\mathrm{Re}}(\xi,t) \equiv \mathcal{P}\int_0^1 \mathrm{d}x\left[\tilde{E}(x,\xi,t) + \tilde{E}(-x,\xi,t)\right]C^-(x,\xi)$$

$$H_{\mathrm{Im}}(\xi,t) \equiv H(\xi,\xi,t) - H(-\xi,\xi,t).$$

$$E_{\mathrm{Im}}(\xi,t) \equiv E(\xi,\xi,t) - E(-\xi,\xi,t)$$

$$\tilde{H}_{\mathrm{Im}}(\xi,t) \equiv \tilde{H}(\xi,\xi,t) + \tilde{H}(-\xi,\xi,t)$$

$$\tilde{E}_{\mathrm{Im}}(\xi,t) \equiv \tilde{E}(\xi,\xi,t) + \tilde{E}(-\xi,\xi,t)$$

with $C^{\pm}(x,\xi) = \frac{1}{x-\xi} \pm \frac{1}{x+\xi}$

JLab Hall A

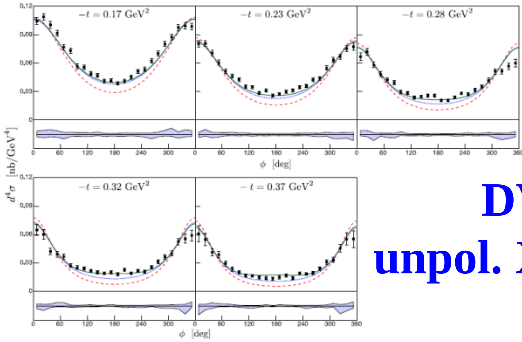

DVCS
unpol. X-section

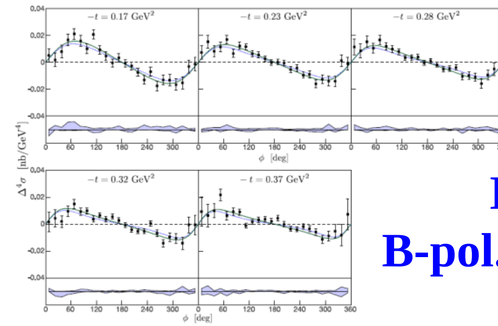

DVCS
B-pol. X-section

JLab CLAS

DVCS
BSA

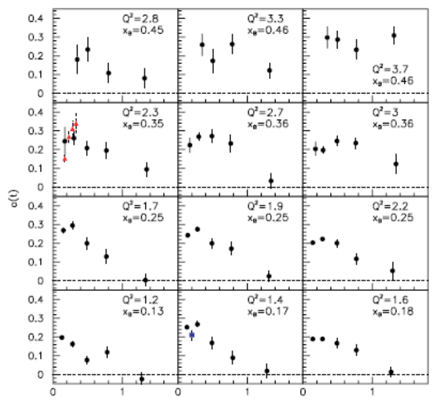

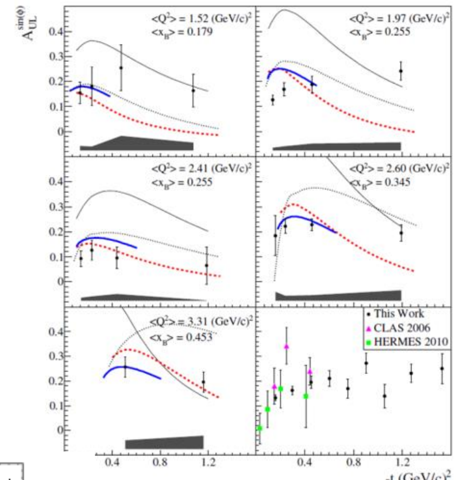

DVCS
lTSA

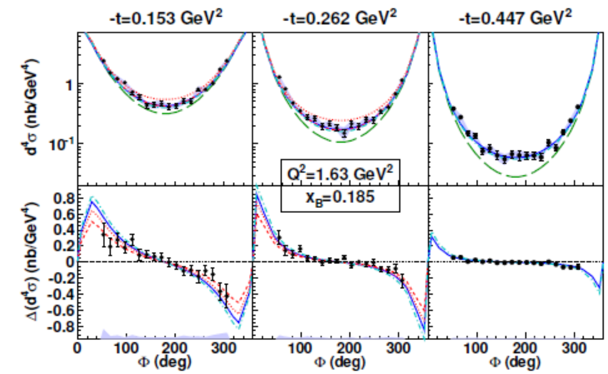

DVCS unpol. and
B-pol. X-sections

HERMES

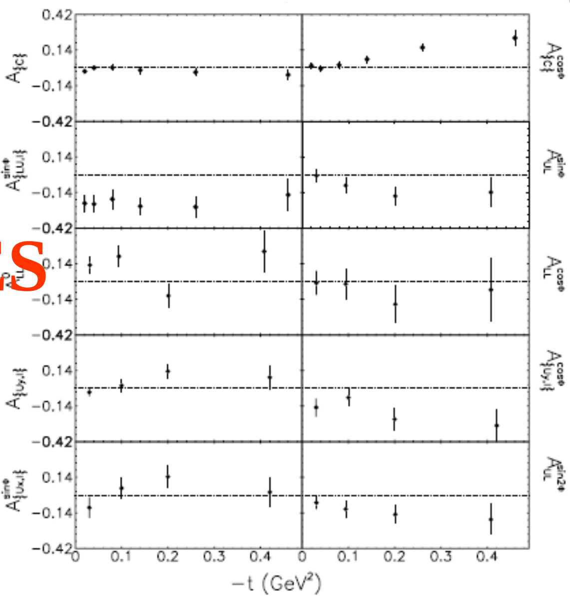

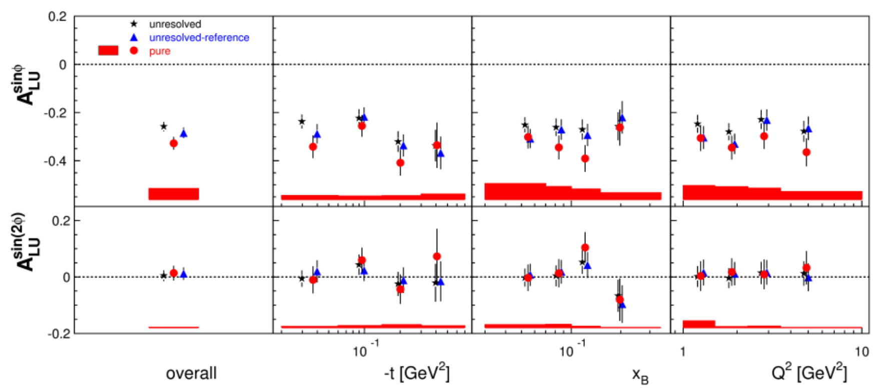

DVCS
BSA,lTSA,tTSA,BCA

Given the well-established LT-LO DVCS+BH amplitude

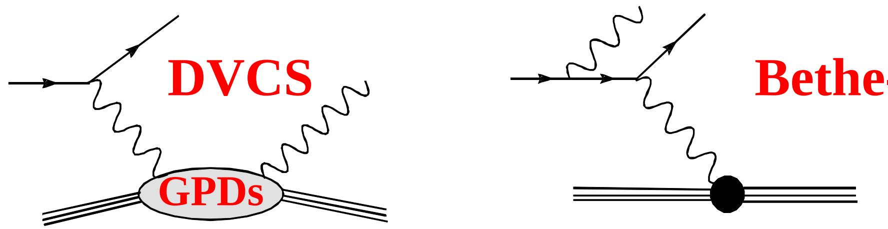

Can one extract the 8 CFFs from the measured observables?

Obs= Amp(DVCS+BH) $\otimes$ CFFs

There are currently **two quasi-model-independent approaches** to extract, at **fixed x_B, t and Q^2** (« **local fitting** »), the CFFs from the DVCS observables

1) Mapping and linearization

If enough observables are measured, one has a **system of 8 equations with 8 unknowns**

Given reasonable **approximations** (leading-twist dominance, neglect of some $1/Q^2$ terms,...), the system can be **linear** (practical for the propagation of errors)

$$\begin{pmatrix} A_{\mathrm{LU,I}}^{\sin(1\phi)} \\ A_{\mathrm{UL,+}}^{\sin(1\phi)} \\ A_{\mathrm{UT,I}}^{\sin(\varphi)\cos(1\phi)} \\ A_{\mathrm{UT,I}}^{\cos(\varphi)\sin(1\phi)} \end{pmatrix} \Rightarrow \Im\mathrm{m} \begin{pmatrix} \mathcal{H} \\ \widetilde{\mathcal{H}} \\ \mathcal{E} \\ \overline{\mathcal{E}} \end{pmatrix}, \qquad \begin{pmatrix} A_{\mathrm{C}}^{\cos(1\phi)} \\ A_{\mathrm{LL,+}}^{\cos(1\phi)} \\ A_{\mathrm{LT,I}}^{\sin(\varphi)\sin(1\phi)} \\ A_{\mathrm{LT,I}}^{\cos(\varphi)\cos(1\phi)} \end{pmatrix} \Rightarrow \Re\mathrm{e} \begin{pmatrix} \mathcal{H} \\ \widetilde{\mathcal{H}} \\ \mathcal{E} \\ \overline{\mathcal{E}} \end{pmatrix}$$

$$\Delta\sigma_{LU} \sim \sin\phi \; \mathrm{Im}\{F_1\mathcal{H} + \xi(F_1+F_2)\widetilde{\mathcal{H}} - kF_2\mathcal{E}\}d\phi$$

$$\Delta\sigma_{UL} \sim \sin\phi \mathrm{Im}\{F_1\widetilde{\mathcal{H}} + \xi(F_1+F_2)(\mathcal{H} + x_B/2\mathcal{E}) - \xi kF_2\,\widetilde{\mathcal{E}} + \ldots\}d\phi$$

K. Kumericki, D. Mueller, M. Murray, Phys. Part. Nucl. 45 (2014) 4, 723

2) «Brute force » fitting

χ^2 minimization (**MINUIT + MINOS**) of the DVCS observables **at a given x_B, t and Q^2 point** by varying the CFFs within a **limited hyper-space** (e.g. 5xVGG)

The problem can be strongly underconstrained:

- **JLab Hall A: pol. and unpol. X-sections**
- **JLab CLAS: BSA + TSA**

2 constraints and 8 parameters !

However, as **some observables are dominated by a single or a few CFFs**, there is a **convergence** (i.e. a **well-defined minimum χ^2**) for those CFFs.

The contribution of the **non-converging CFF** enters in the **error bar** of the converging ones. For instance (naive):

$3 = y + 0.001x$ **If $-10<x<10$:** $3 = y \pm 0.01 \ (\text{or } y = 3 \pm 0.01)$

M. Guidal, EPJA 37 (2008) 319 **M.G., PLB 689 (2010) 156** **M.G., PLB 693 (2010) 17**
M.G. & H. Moutarde, EPJA 42 (2009) 71 **M.G. & M. Boer, J.Phys.G 42 (2015) 034023**

Cross-check of the two local GPD-extraction methods

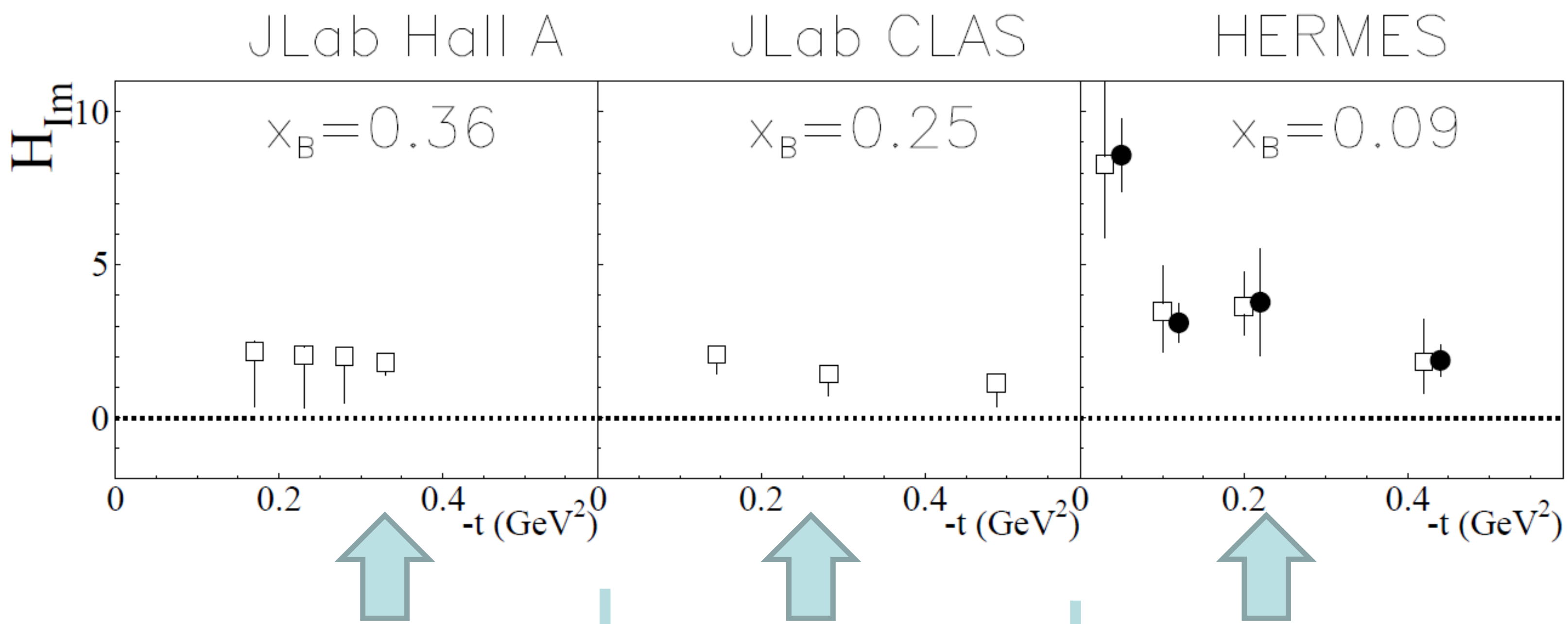

unpol. cross sec.	beam spin asymm.	beam charge asymm.
+	+	+
beam pol. cross sec.	long. pol. tar. asymm.	beam spin asymm.
(2006)	(2008, 2006)	+
		…

□ χ^2 minimization

● linearization

M. G., H. Moutarde, M. Vanderaeghen, Rept. Prog. Phys. 76 (2013) 066202

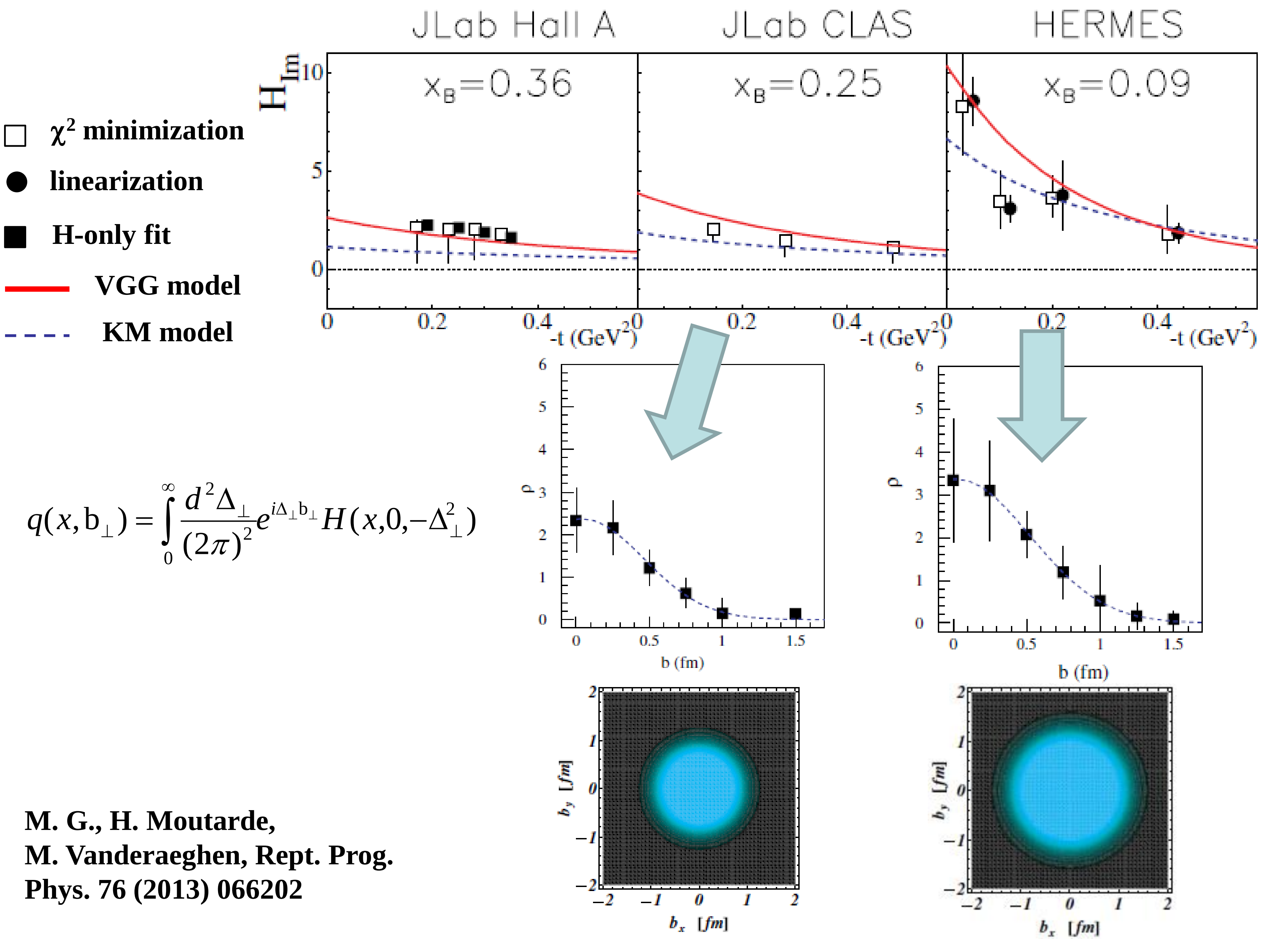

$$q(x,\mathrm{b}_\perp)=\int_0^\infty \frac{d^2\Delta_\perp}{(2\pi)^2} e^{i\Delta_\perp \mathrm{b}_\perp} H(x,0,-\Delta_\perp^2)$$

M. G., H. Moutarde, M. Vanderaeghen, Rept. Prog. Phys. 76 (2013) 066202

Examples of correlation between H_{Im} and $\tilde{H}_{Im}$

Fitting only 2 observables: $\Delta\sigma_{LU}$ & σ (Hall A)

Contour plots for different fit starting values, two kinematics

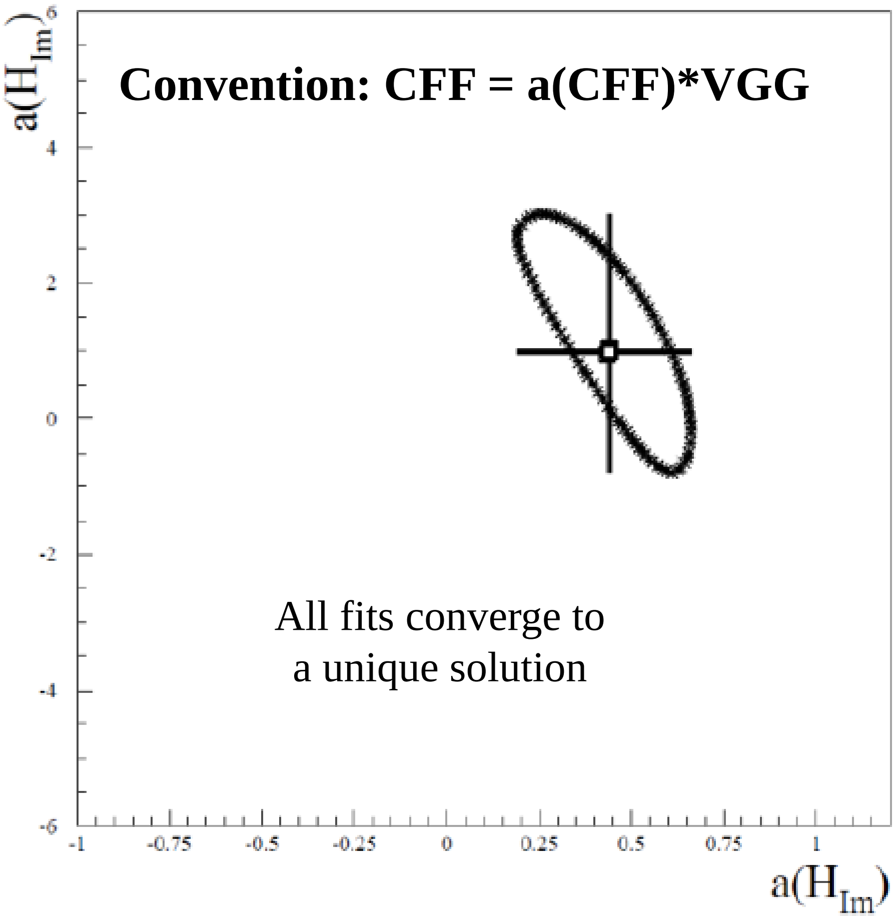

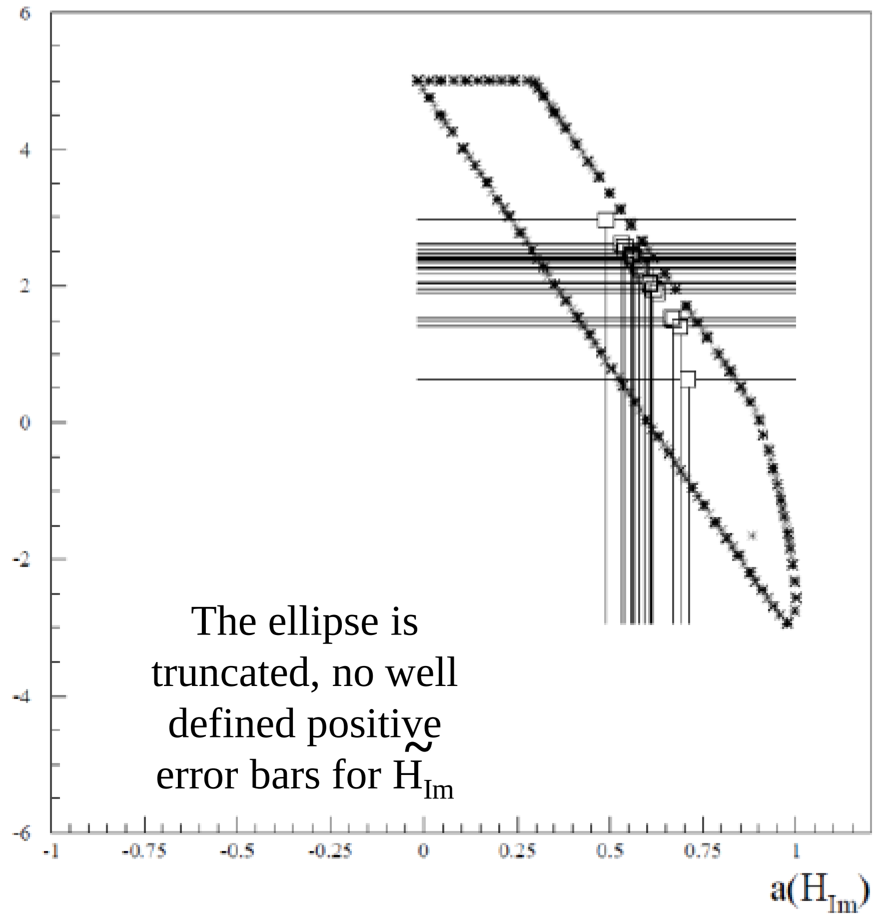

Polarized beam, unpolarized target **(BSA)** :

$\Delta\sigma_{LU} \sim \sin\phi \, \mathrm{Im}\{F_1\mathcal{H} + \xi(F_1+F_2)\tilde{\mathcal{H}} - kF_2\mathcal{E}\}d\phi$

R. Dupré, M. Guidal, S.Niccolai, M. Vanderhaegen, arXiv: 1704.07330

Systematic checks on pseudo data: error bars prescription

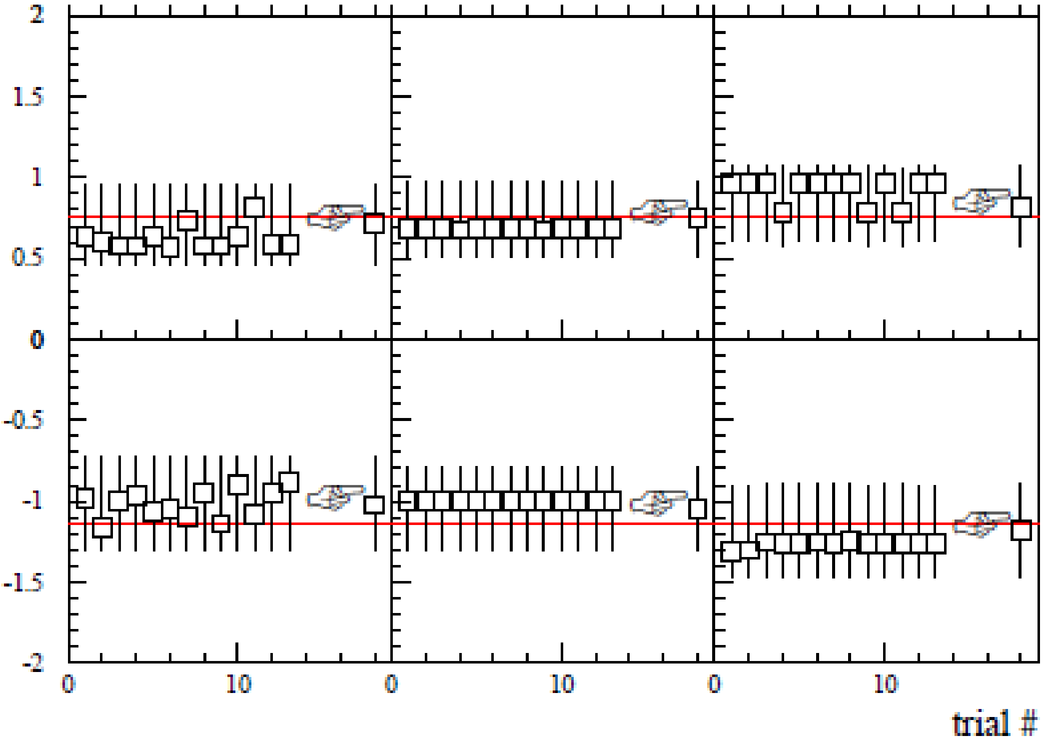

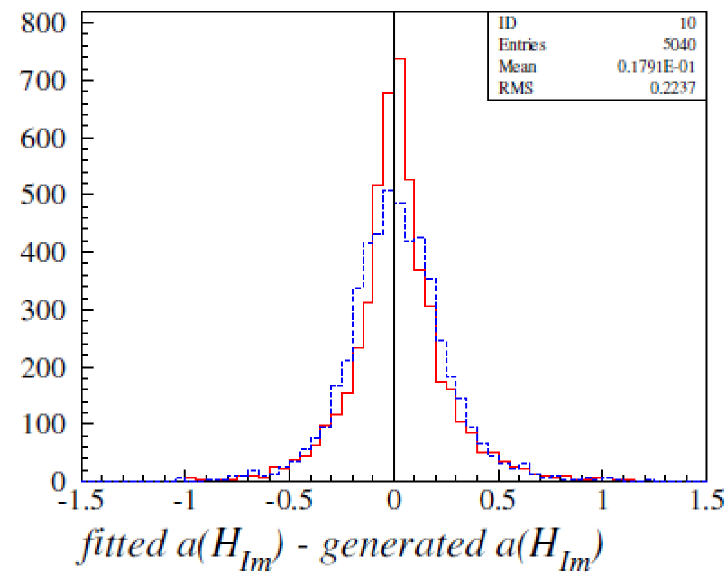

Results for a(H_{im}) of many fits differing by their **starting values** (« trial »), for different sets of randomly **generated CFFs** (rows), and for different random **smearings of the pseudo-data** (columns)

- Difference between the « middle value » for a, calculated from the largest error bars of all solutions
- Difference between the χ^2_{min} solution and the generated vallue

Recent data from JLab

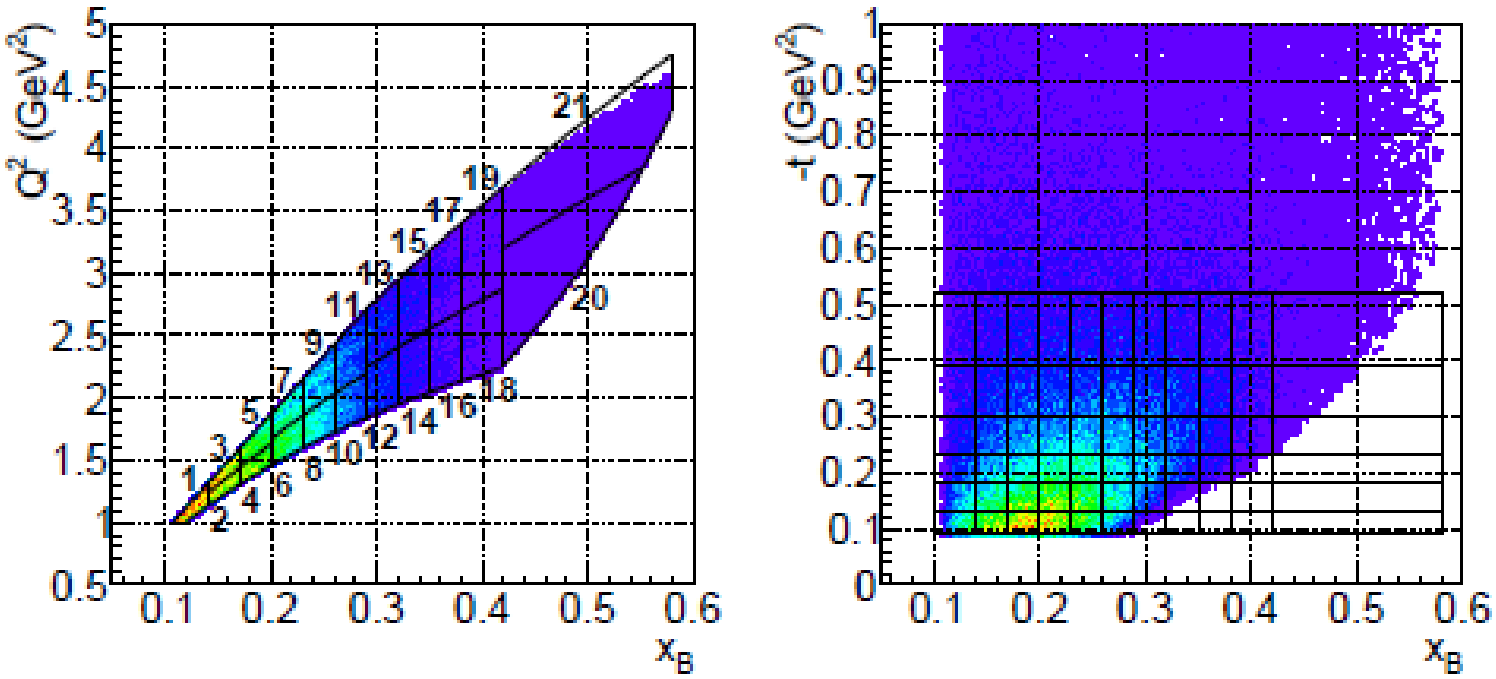

Hall A, PRC92 (2015), 055202: unpol. and beam-pol. cross sections

High precision - 20 bins

CLAS, PRL 114 (2015), 032001: longitudinal TSA

CLAS, PRD91 (2015), 052014: BSA, lTSA, DSA

Polarized target, 3 observables - 20 bins

CLAS, PRL 115 (2015), 212003: unpol. and beam-pol. cross sections

Wide coverage - > 100 bins

Results for H_{Im} and $\tilde{H}_{Im}$ from the fits of JLab 2015 data

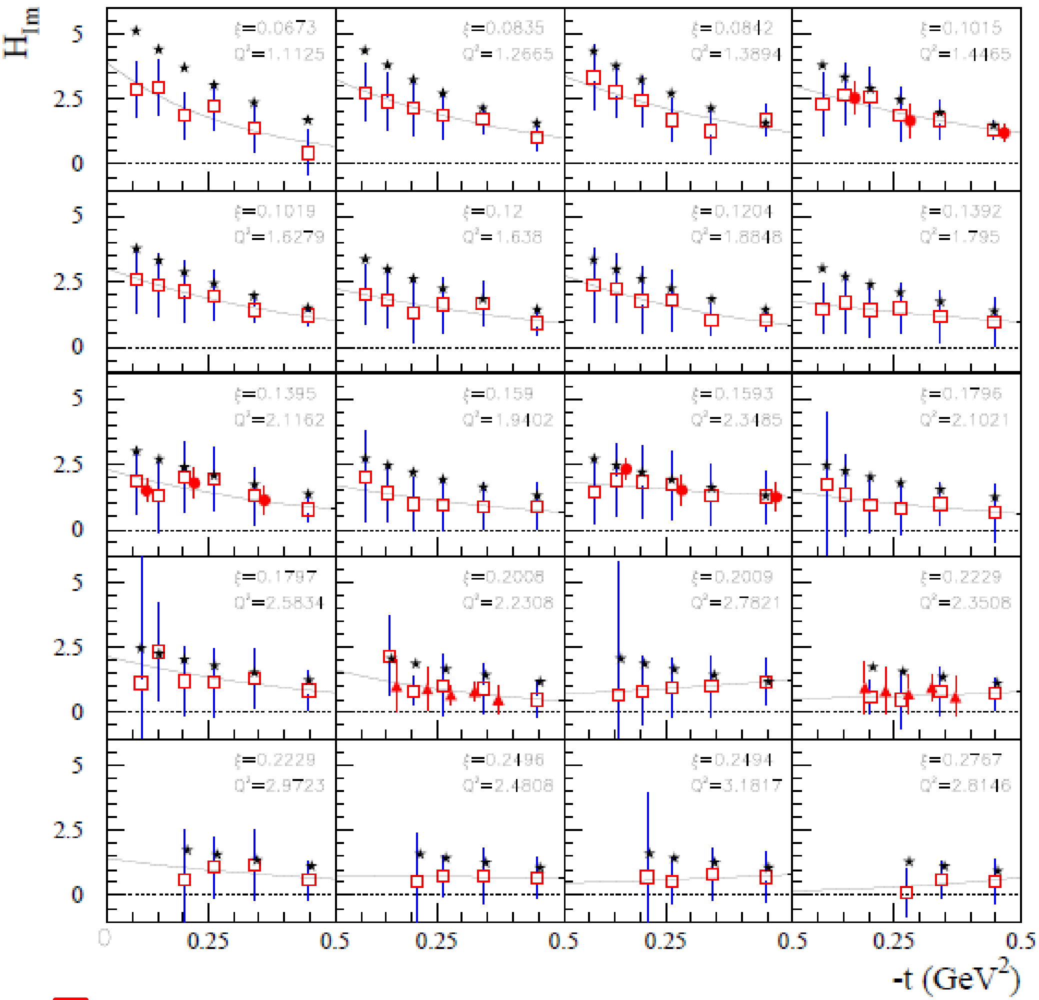

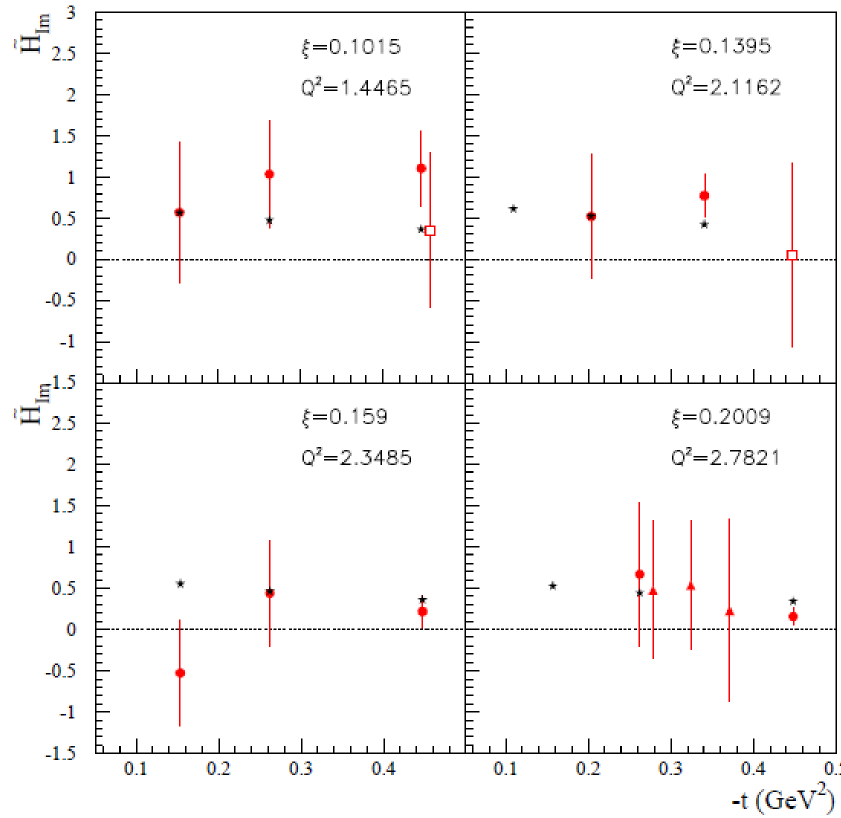

H_{Im} has steeper t-slope than $\tilde{H}_{Im}$: the axial charge is more "concentrated" than the electric charge

- Fit to CLAS c.s. and beam pol. c.s.
- Fit to CLAS c.s., beam pol. c.s., lTSA, DSA
- Fit to Hall A c.s. and beam pol. c.s.
- VGG model

From CFFs to proton tomography

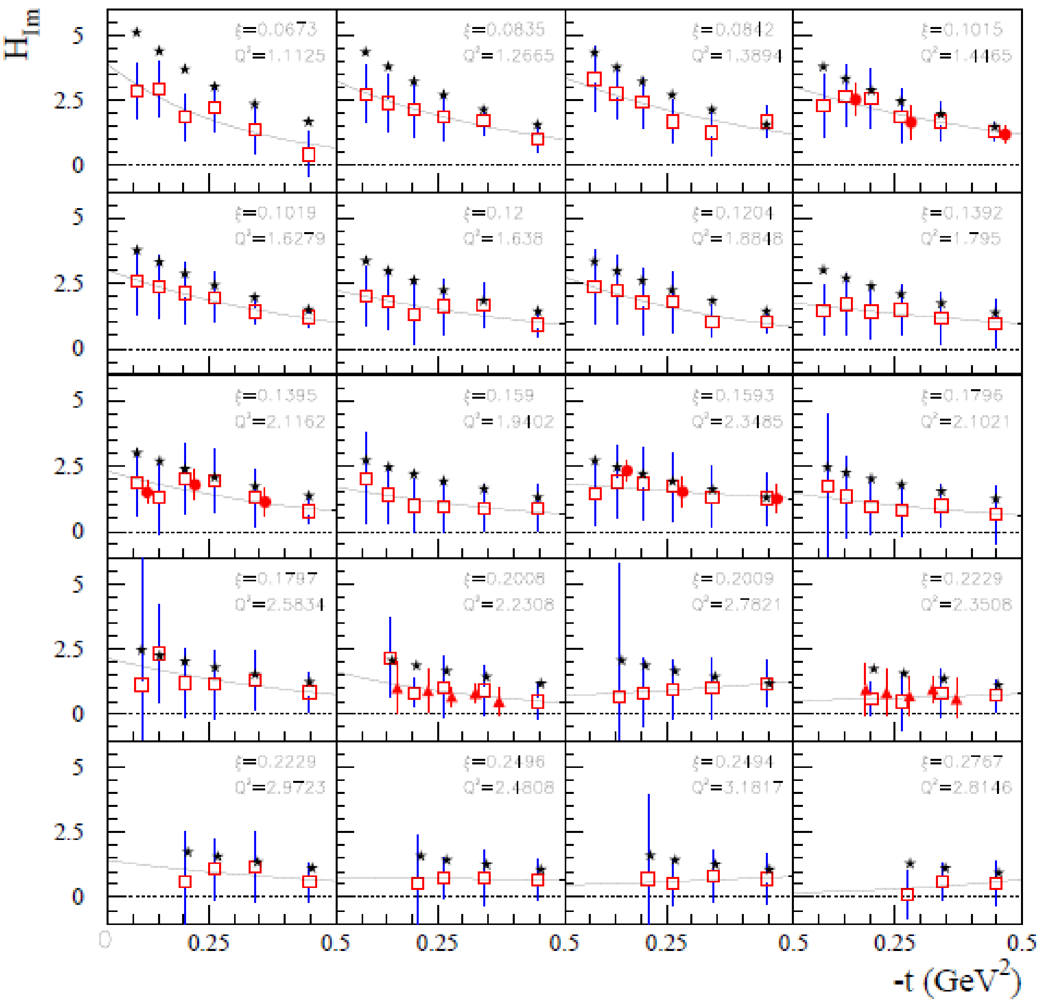

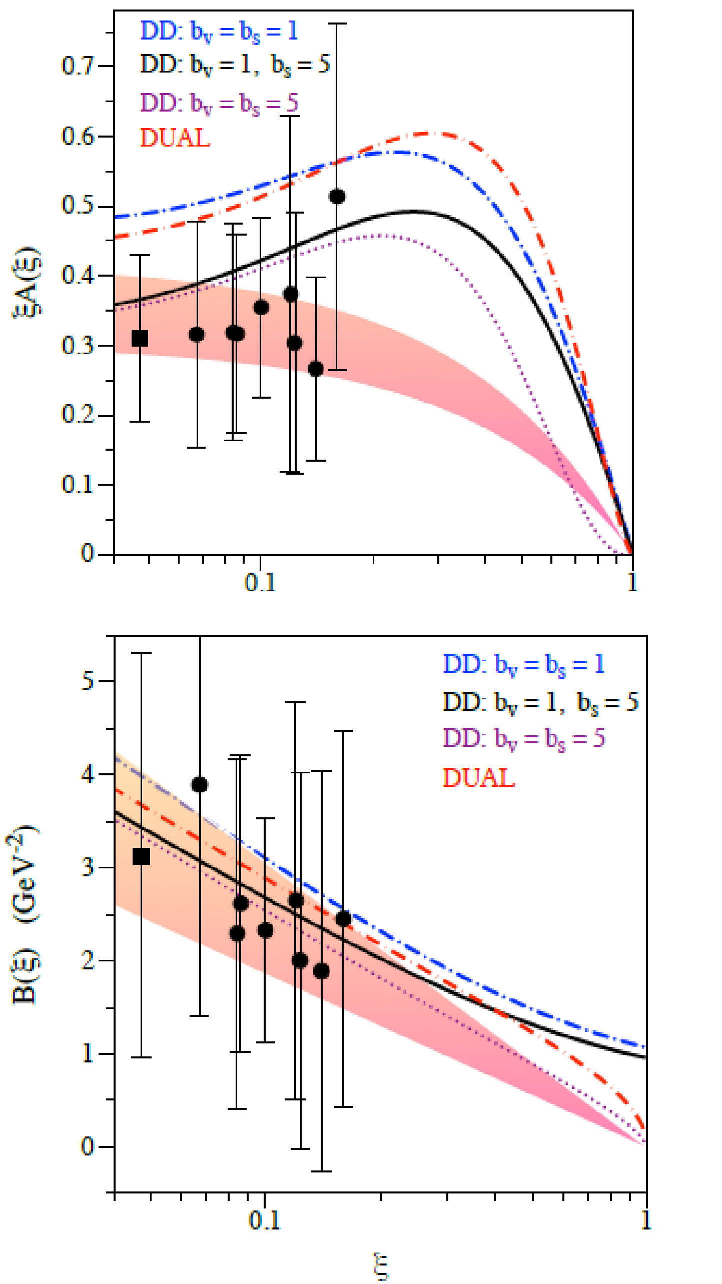

$$\mathcal{H}_{Im}(\xi, t) = A(\xi) e^{B(\xi)t}$$

$$A(\xi) \;=\; a_A(1-\xi)/\xi \qquad a_A = 0.36 \pm 0.06$$

$$B(\xi) = a_B \ln(1/\xi) \qquad a_B \;=\; 1.07 \pm 0.26 \text{ GeV}^{-2}$$

From CFFs to proton tomography

$$\rho^q(x, \mathbf{b}_\perp) = \int \frac{d^2\boldsymbol{\Delta}_\perp}{(2\pi)^2} e^{-i\mathbf{b}_\perp\cdot\boldsymbol{\Delta}_\perp} H^q_-(x, 0, -\boldsymbol{\Delta}_\perp{}^2) \qquad \langle b_\perp^2\rangle^q(x) = -4\frac{\partial}{\partial\boldsymbol{\Delta}_\perp^2} \ln H^q_-(x, 0, -\boldsymbol{\Delta}_\perp{}^2)\Big|_{\boldsymbol{\Delta}_\perp=0}$$

If $\quad H^q_-(x, 0, t) = q_v(x)e^{B_0(x)t} \Rightarrow \langle b_\perp^2\rangle^q(x) = 4B_0(x)$

However, this formula involves: $\quad H^q_-(x, 0, t) \equiv H^q(x, 0, t) + H^q(-x, 0, t)$

While we extract: $\quad H^q_+(x, \xi, t) \equiv H^q(x, \xi, t) - H^q(-x, \xi, t)$

$\Rightarrow$ **Need to estimate:** $B_0(x)/B(x)$ (assuming $H^q_-(x, 0, t) = q_v(x)e^{B_0(x)t}$)

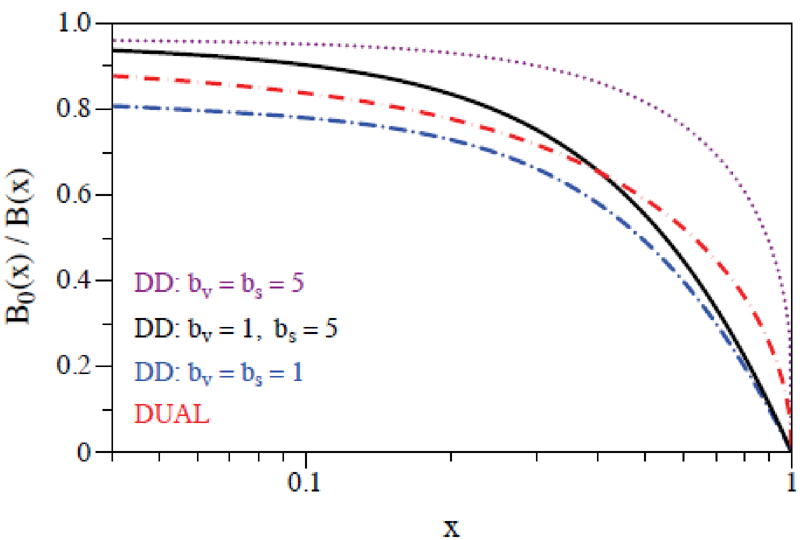

$0.90 < B_0/B < 0.95$ for $0.05 \lesssim x \lesssim 0.2$

$\Rightarrow B_0/B \simeq 0.925 \pm 0.025$

From CFFs to proton tomography

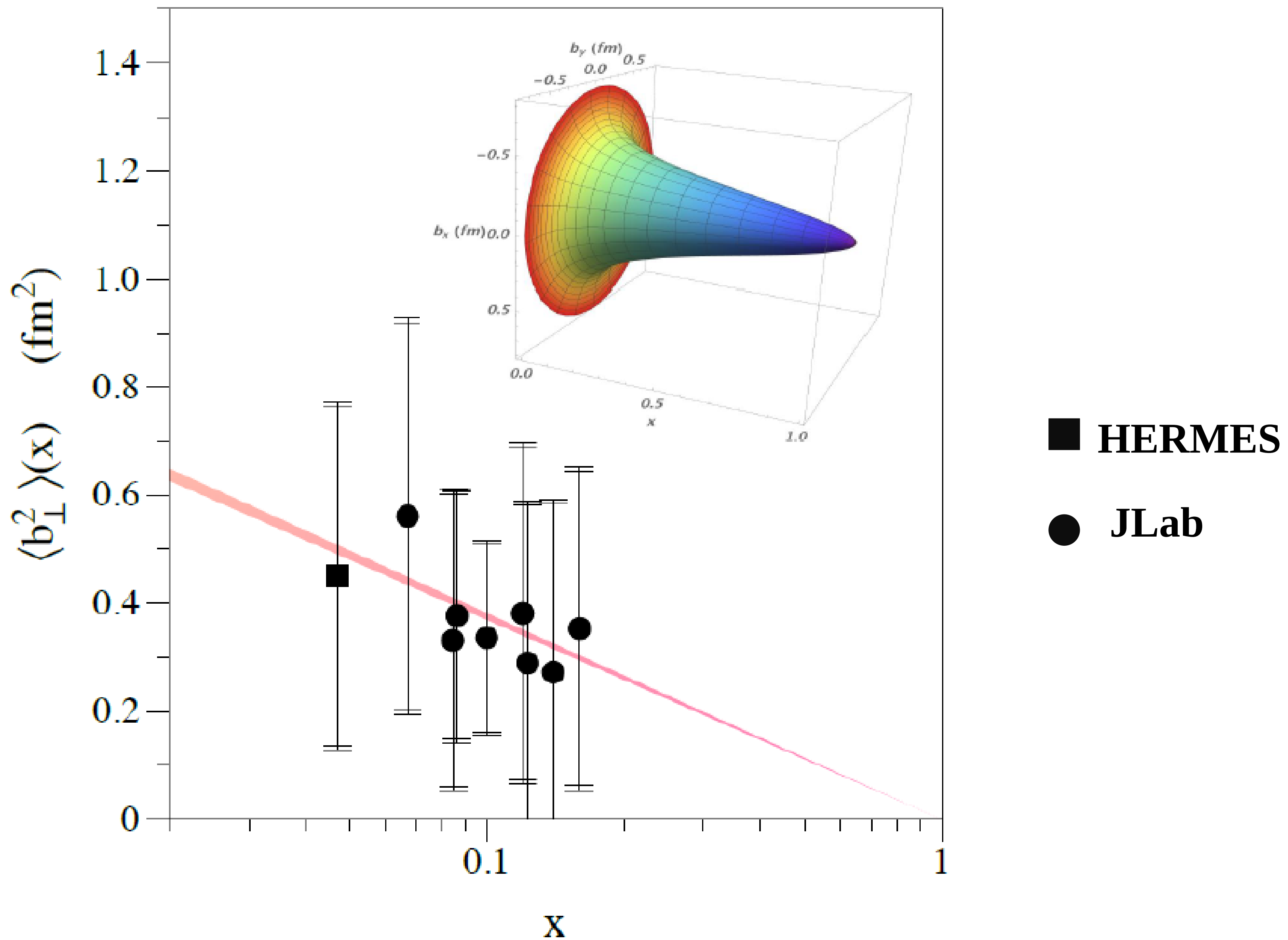

« Integrated » radius from elastic form factor F1: $\langle b_\perp^2 \rangle = 0.43 \pm 0.01 \ \mathrm{fm}^2$

Dispersion relations

$$H_{Re}(\xi,t) = -\Delta(t) + \mathcal{P}\int_0^1 dx\, H_+(x,x,t)\, C^+(x,\xi)$$

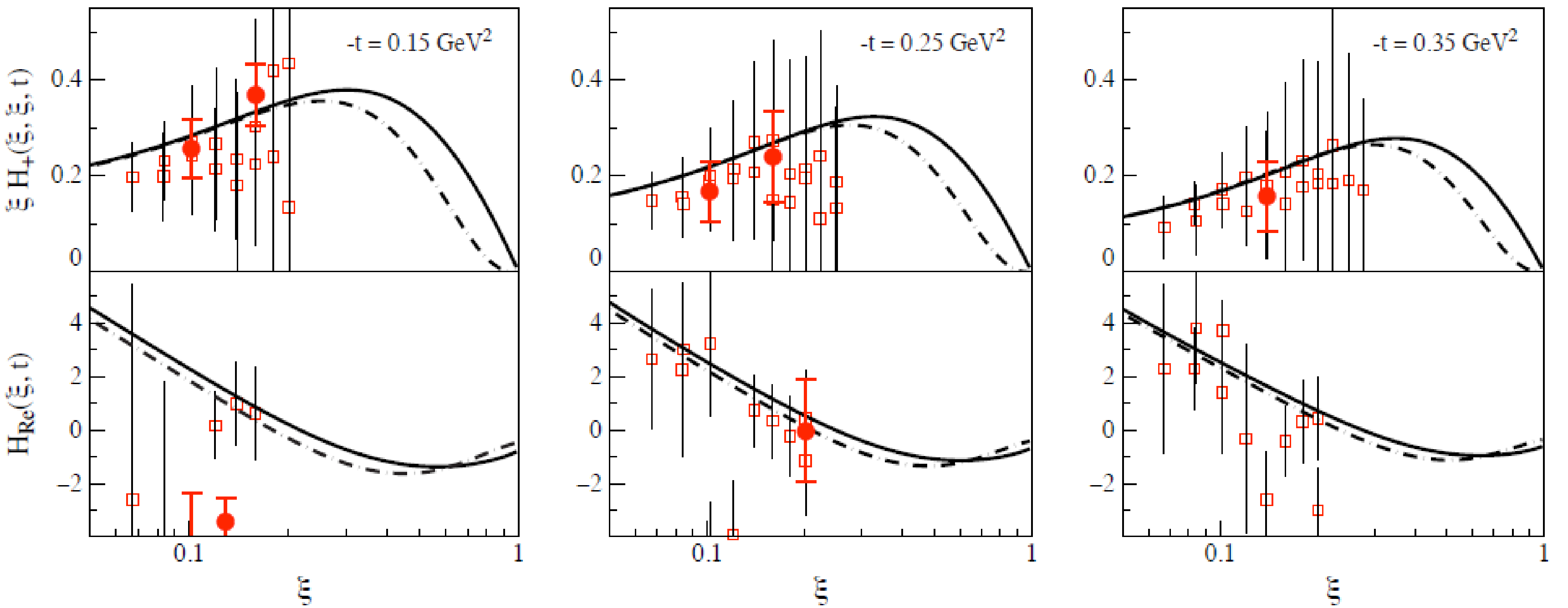

Fig. 26. Comparison of the ξ dependence of the imaginary parts (upper plots) and real parts (lower plots) of the CFF related to the GPD H for the proton for three values of t. The curves in the upper plots are based on two DD parameterizations. Solid curves: DD parameterization with $b_v = 1$ and $b_s = 5$; dashed curves: DD parameterization with $b_v = 5$ and $b_s = 5$. The curves in the lower plots are the dispersive calculations of the real parts according to Eq. (38), based on the input of the imaginary parts from the upper plots, and with subtraction function $\Delta(t)$ set equal to zero. Open squares: results of the CLAS σ and $\Delta\sigma_{LU}$ fit. Solid circles: results of the fit to CLAS σ, $\Delta\sigma_{LU}$, A_{UL}, and A_{LL} data.

GPDs: where we stand, where we go

GPDs contain a **wealth of information** on nucleon structure and dynamics: space-momentum quark correlation, orbital momentum, pressure forces within the nucleon,…

First new insights of nucleon structure (x-dependence of the charge radius, electric vs. axial charge) are already emerging from the HERMES and recent JLab data, thanks to **new fitting algorithms**

Large flow of new observables and new data expected soon (JLab6, JLab12, COMPASS)

Other DVCS-related measurements planned for JLab 12 GeV (nDVCS, TCS, DDVCS)

CLAS12: projections for flavor separation ($Im\mathcal{H}$, $Im\mathcal{E}$)

$$(H,E)_u(\xi,\xi,t) = \tfrac{9}{15}\left[4(H,E)_p(\xi,\xi,t) - (H,E)_n(\xi,\xi,t)\right]$$

$$(H,E)_d(\xi,\xi,t) = \tfrac{9}{15}\left[4(H,E)_n(\xi,\xi,t) - (H,E)_p(\xi,\xi,t)\right]$$

$$\frac{1}{2}\int_{-1}^{1} x dx \left(H^q(x,\xi,t=0) + E^q(x,\xi,t=0)\right) = J^q$$

Fits done to all the projected observables for **pDVCS** (BSA, lTSA, lDSA, tTSA, CS, DCS) and **nDVCS** (BSA,lTSA, lDSA) of the CLAS12 program

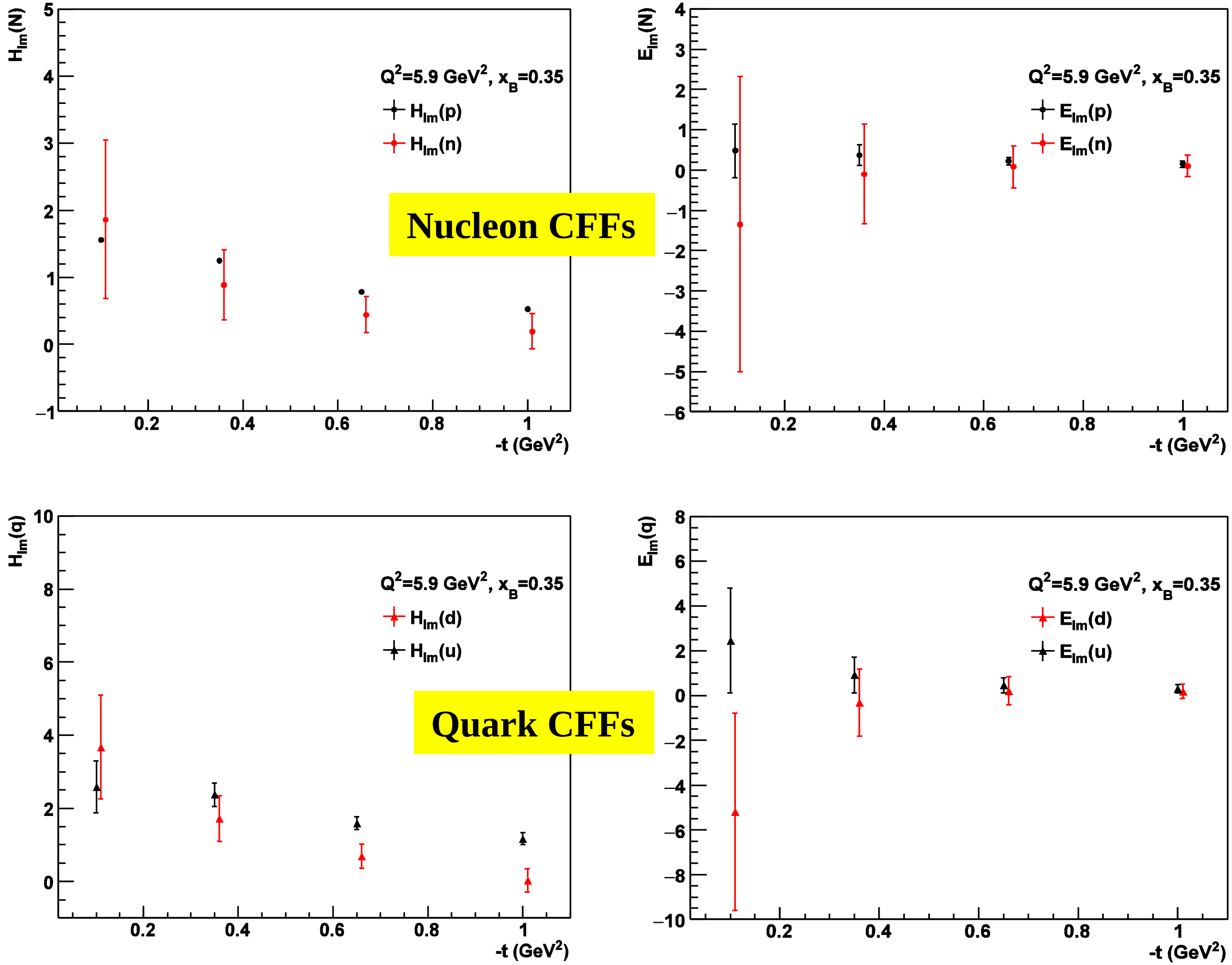

Global outlook: DVCS past, present and future

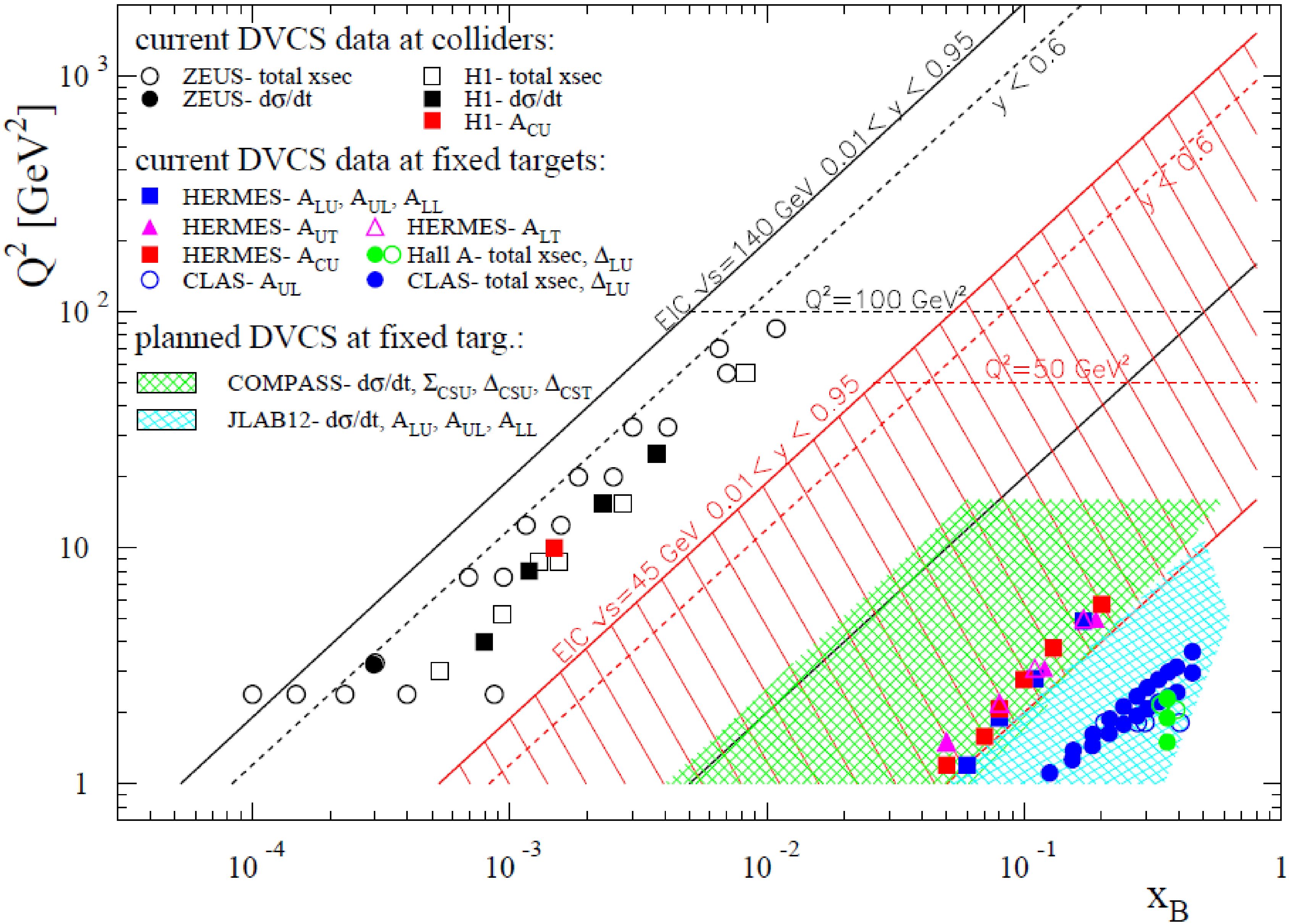

Back-up slides

The Bethe-Heitler process

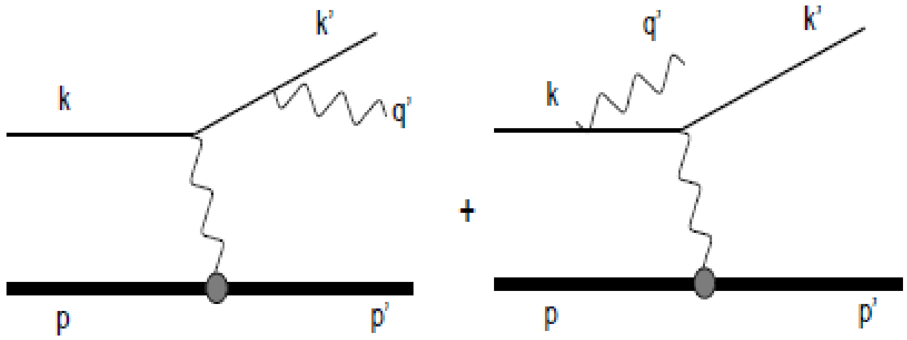

$$T^{BH} = \frac{-e^3}{t} \varepsilon'^{*}_{\mu} L^{\mu\nu} \, \overline{u}(p') \Gamma_{\nu}(p', p) u(p)$$

$$L^{\mu\nu} = \overline{u}(k') \left(\gamma^{\mu} \frac{1}{\gamma.(k' + q') - m_e + i\epsilon} \gamma^{\nu} + \gamma^{\nu} \frac{1}{\gamma.(k - q') - m_e + i\epsilon} \gamma^{\mu} \right) u(k)$$

$$\Gamma^{\nu}(K', K) \quad = \quad \boxed{F_1(X)} \gamma^{\nu} + i \boxed{F_2(X)} \sigma^{\nu\rho} (K' - K)_{\rho} / 2m$$

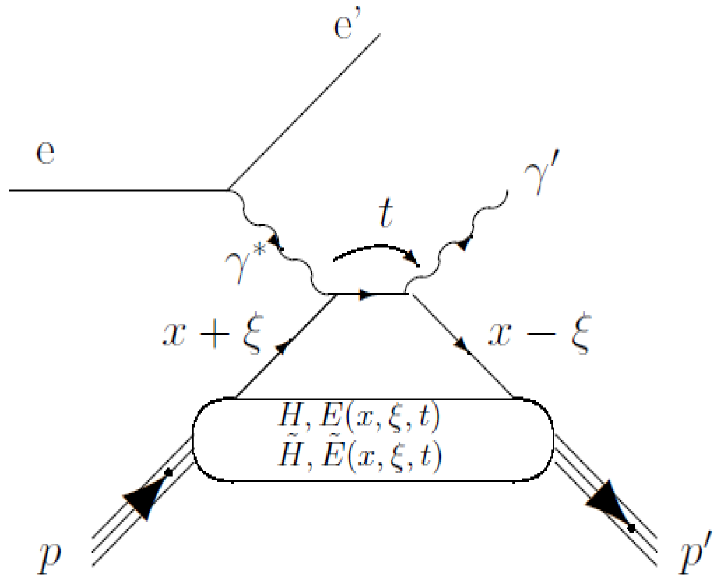

$$
\begin{aligned}
&H^{\mu\nu}_{L.O.DVCS} \\
&= \frac{1}{2}\left[\tilde{p}^{\mu}n^{\nu}+\tilde{p}^{\nu}n^{\mu}-g^{\mu\nu}\right]\int_{-1}^{+1}dx\left[\frac{1}{x-\xi+i\epsilon}+\frac{1}{x+\xi-i\epsilon}\right] \\
&\quad\times\left[\boxed{H^{p}_{DVCS}}(x,\xi,t)\;\bar{N}(p')\gamma.nN(p)+\boxed{E^{p}_{DVCS}}(x,\xi,t)\;\bar{N}(p')i\sigma^{\kappa\lambda}\frac{n_{\kappa}\Delta_{\lambda}}{2m_N}N(p)\right] \\
&+\;\frac{1}{2}\left[-i\varepsilon^{\mu\nu\kappa\lambda}\tilde{p}_{\kappa}n_{\lambda}\right]\int_{-1}^{+1}dx\left[\frac{1}{x-\xi+i\epsilon}-\frac{1}{x+\xi-i\epsilon}\right] \\
&\quad\times\left[\boxed{\tilde{H}^{p}_{DVCS}}(x,\xi,t)\bar{N}(p')\gamma.n\gamma_5N(p)+\boxed{\tilde{E}^{p}_{DVCS}}(x,\xi,t)\bar{N}(p')\gamma_5\frac{\Delta\cdot n}{2m_N}N(p)\right]\;,
\end{aligned}
$$

$$
T^{DVCS}\sim\int_{-1}^{+1}\frac{H(x,\xi,t)}{x\pm\xi+i\varepsilon}dx+\ldots\sim\quad P\int_{-1}^{+1}\frac{H(x,\xi,t)}{x\pm\xi}dx-i\pi H(\pm\xi,\xi,t)+\ldots
$$

$H^q(x,\xi,t)$ but only ξ and t experimentally accessible

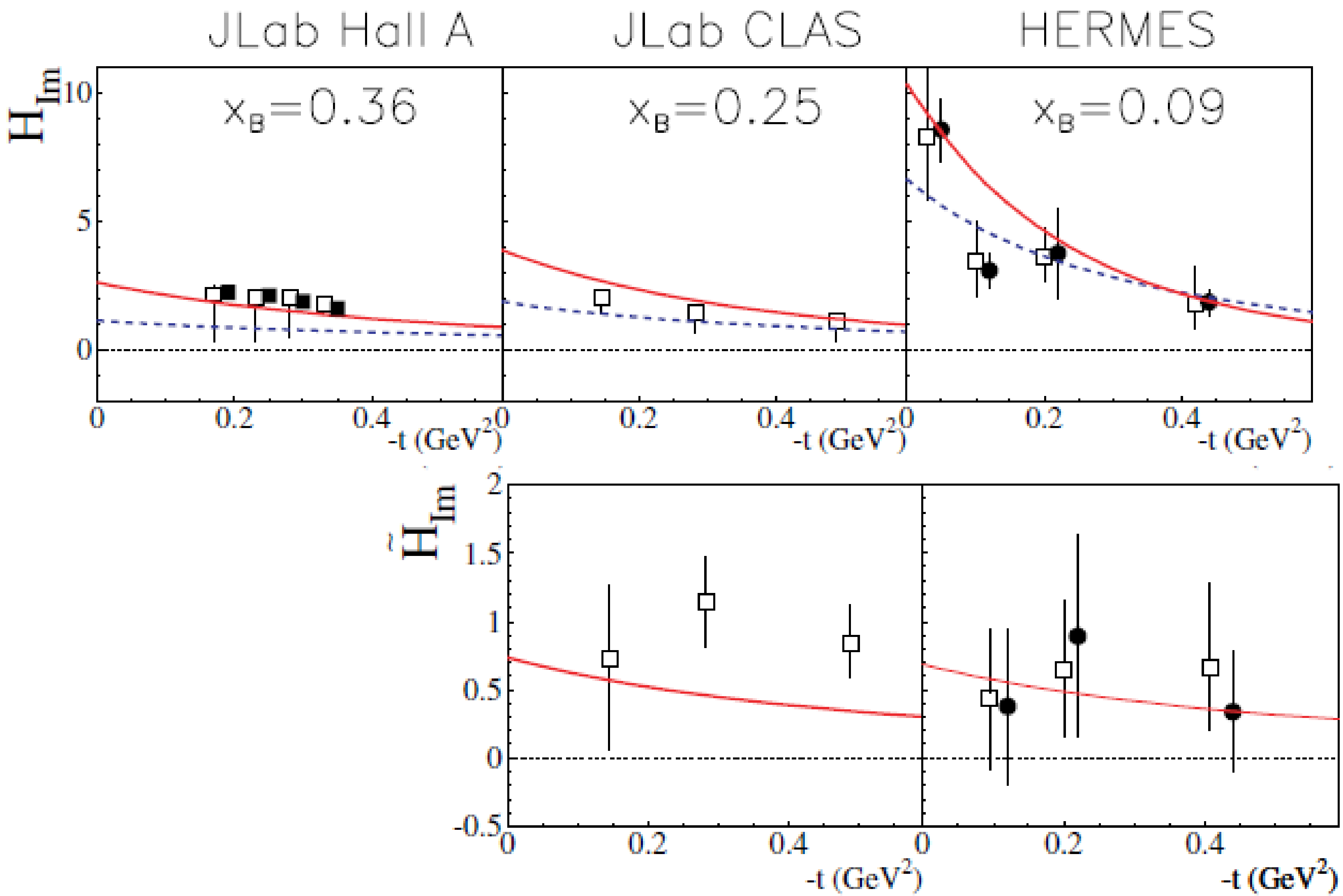

The axial charge (H_{im}) appears to be more « concentrated » than the electromagnetic charge ($\tilde{H}_{im}$)

Confirmed by new CLAS A_UL and A_LL data:

Phys.Rev. D91 (2015) 5, 052014

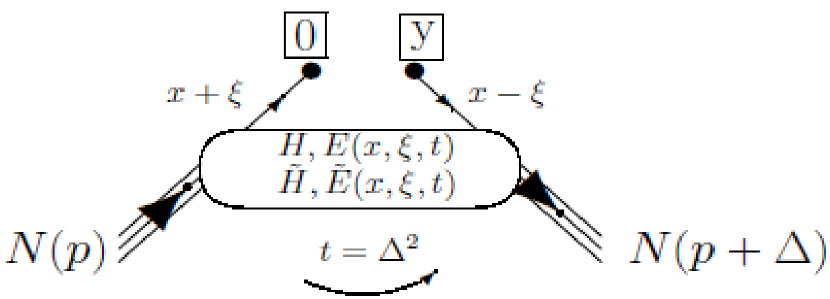
0
y
$x+\xi$
$x-\xi$
$H, E(x,\xi,t)$
$\tilde{H}, \tilde{E}(x,\xi,t)$
$N(p)$
$N(p+\Delta)$
$t=\Delta^2$

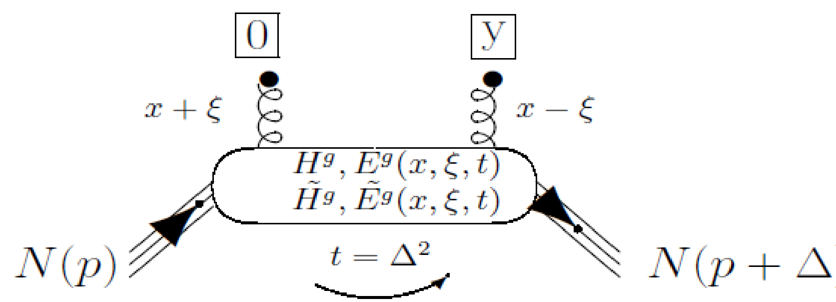
0
y
$x+\xi$
$x-\xi$
$H^g, E^g(x,\xi,t)$
$\tilde{H}^g, \tilde{E}^g(x,\xi,t)$
$N(p)$
$N(p+\Delta)$
$t=\Delta^2$

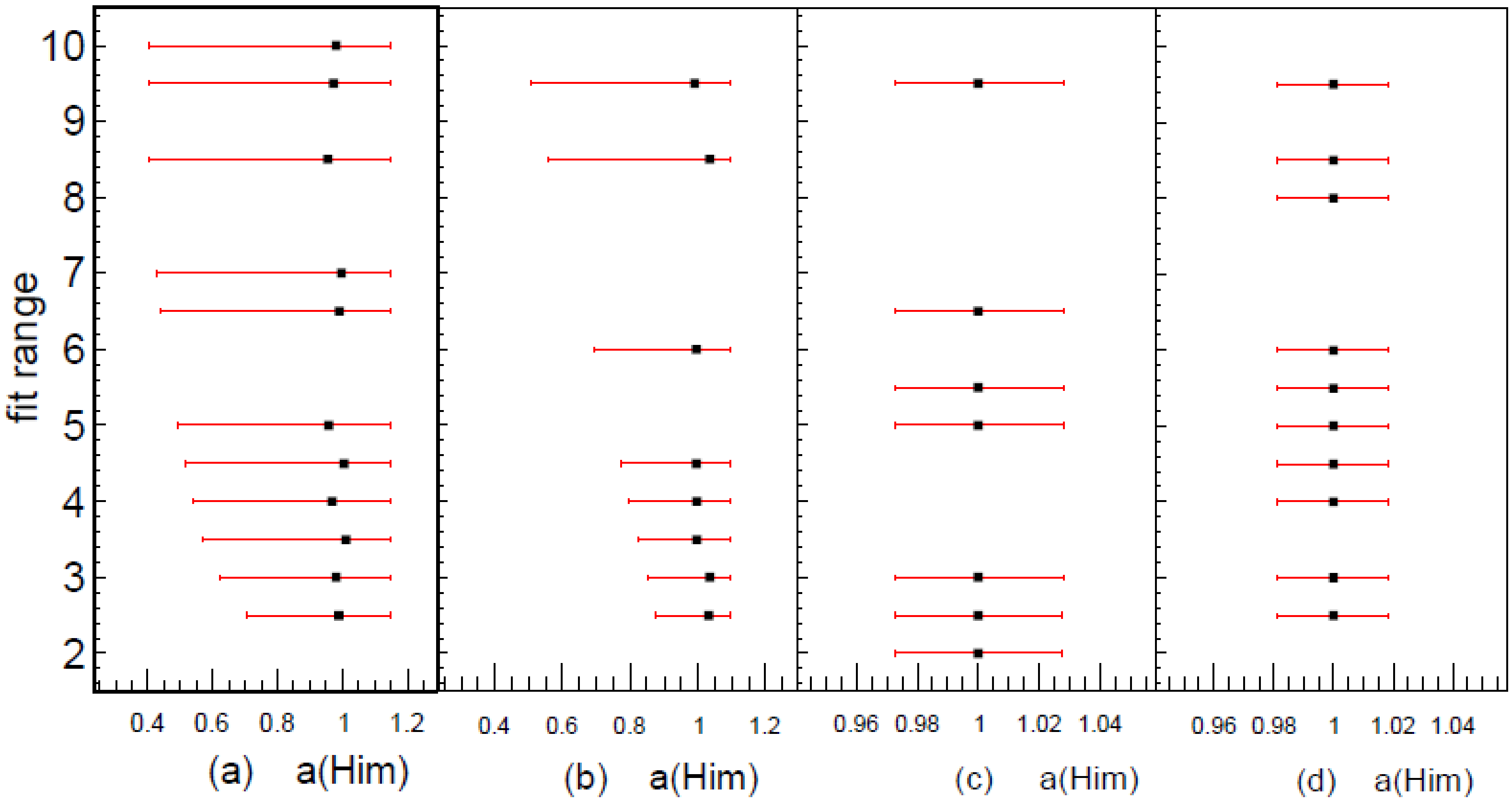

M. Boer, MG J.Phys. G42 (2015) 3, 034023

Figure 5. Results of fits based on simulations for the CFF multiplier $a(H_{Im})$ and its error bar (x-axis) for different maximum ranges of the domain of variation allowed for the CFFs (y-axis, in units of VGG CFFs) and for different sets of observables fitted: (a) the unpolarized cross section σ and the beam-polarized cross section $\Delta\sigma_{LU}$ (like the Hall A data), (b) σ, $\Delta\sigma_{LU}$ and $\Delta\sigma_{Uz}$, (c) σ, $\Delta\sigma_{LU}$, $\Delta\sigma_{Uz}$, $\Delta\sigma_{Ux}$ and $\Delta\sigma_{Uy}$, (d) σ and all single and double polarization observables. The pseudo-data that were fitted were generated with the VGG values, so that the multipliers of all CFFs should be 1. In this example, the kinematics is approximately similar to the JLab Hall A data: xi=0.2, Q^2=3 GeV^2 and $-t$=0.4 GeV^2.